Proceedings of the 2nd International Conference on Computing Innovation and Applied Physics
DOI: 10.54254/2753-8818/19/20230517

# Emergent phenomena in quantum phase transition

**Yidi Wang**

School of Physical Sciences, University of Science and Technology of China, 96 JinZhai Road Baohe District, Hefei, Anhui, 230026, P.R.China

yidi0820@mail.ustc.edu.cn

**Abstract**. Emergent phenomena near the quantum critical point at sufficiently low temperature attracts accumulating attentions with respect to both theories and applications. On the contrary to materials with itinerant electrons, ferroelectric materials are relatively less studied but promising in studying novel quantum orders. In this report, we focus on one clean model system, strontium titanite oxide, to explore the quantum criticality. The stabilization of a quantum paraelectric phase has been verified by the previous experimental observation of the dielectric permittivity saturating at a rather high value to the order of $10^4$ under 4 Kelvin. To understand the underlying mechanism, we apply the quantum generalization of Ginzburg-Landau theory as well as lattice dynamics, i.e., the stiffness of soft phonon mode to rationalize the deviation from the classical paraelectric to ferroelectric phase transitions. Besides, under the effective upper critical dimension, a logarithmic correction of the relationship between relative permittivity $\varepsilon$ and temperature $T$ could explain the upturn found in $\varepsilon \sim T^{-1}$ diagram.

**Keywords:** quantum phase transition,ferroelectricity,strontium titanite,critical behaviours.

## 1. Introduction

The study of classical phase transition lays the foundation of thermal dynamics and propels long-distance transportation, cooling techniques, and so on. However, as the temperature ($T$) goes down, theories based on thermal fluctuations and quantum fluctuations at 0 Kelvin (Fermi liquid theory, for instance) fail to explain the emergent phenomena, such as high-temperature superconductivity in cuprates [1](figure 1 (a)), charge density wave in Kagome metals [2] (figure 1 (b)), non-Fermi liquid behaviors in heavy fermion systems, metallic ferromagnetism [3,4](figure 1 (c)), and quantum paraelectricity in $SrTiO_3$ [4-6], $BiFeO_3$ [2], etc. These phenomena have vast potential applications, including electricity transportation [7], satellite memories [7], quantum computation [8] and quantum annealing [9]. In the process of studying these behaviors and trying to broaden their scope of use, the concept of quantum phase transition is established, enriched, and then widely employed in the past decades.

DOI: 10.54254/2753-8818/19/20230517

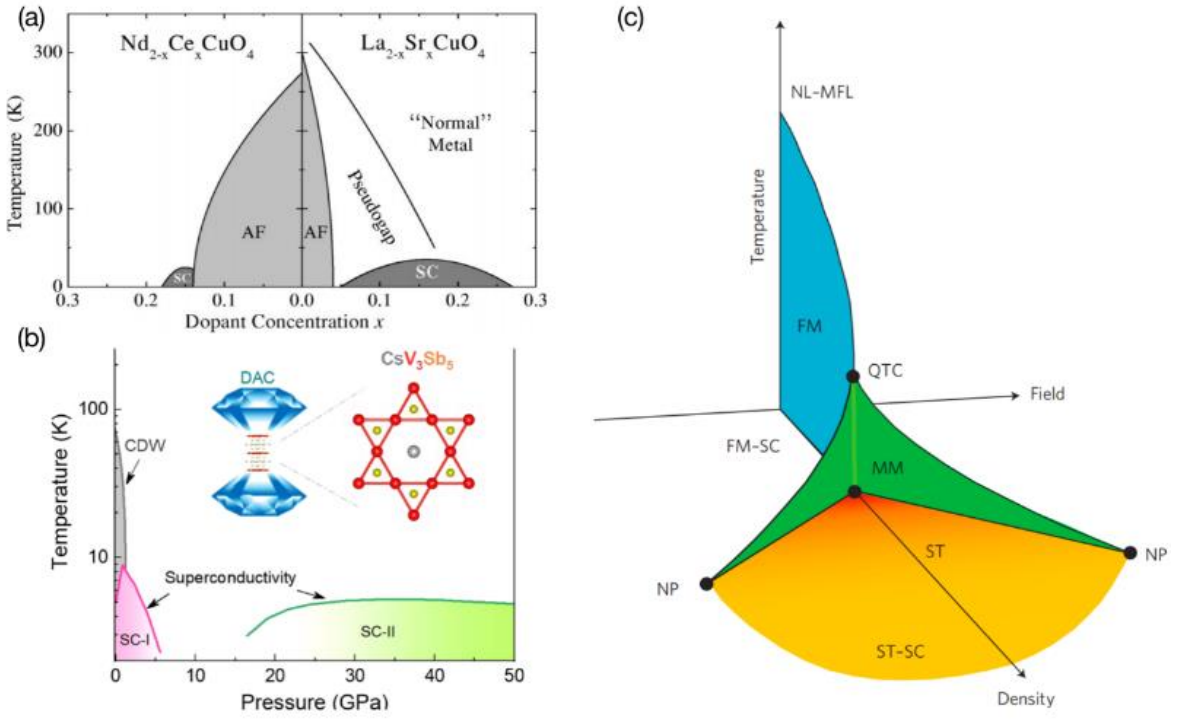


**Figure 1.** Selected phase diagrams of emergent phenomena of quantum phase transition. (a) Electron- and hole-doped high-temperature superconductors [1]. AFM = antiferromagnetism, SC = superconductivity. (b) Pressure-induced phase transition of topological Kagome metal $CsV_3Sb_5$ [2]. CDW = charge density wave. (c) Quantum criticality on the border of ferromagnetism (FM) in $UGe_2$ [3,4].

### *1.1. Quantum phase transition*

Descriptions and Phase Diagrams. Quantum phase transition (QPT) happens as a result of quantum fluctuations which destroy long-range order. At absolutely 0K, phase transition is achieved by exciting the ground state via tuning an external parameter such as pressure, applied electric or magnetic field, chemical doping, strain, etc. In the continuous QPT, the system transits from the ground state to the tuned order, crossing a critical value of external parameter which is defined as the quantum critical point (QCP). However, when extended to low $T$ region, QPT is attributed to both quantum and thermal fluctuations [10]. As is shown in figure 2, for materials with ordered state above 0K, a classical phase transition will happen under a particular value of external parameter; Yet changing the tuning parameter to another value could set the system into a novel quantum ordered state within a broad range of $T$. Hence, there exists a region where thermal and quantum effects are of comparable importance. This region, extended from QCP, is called the quantum critical region.

In the vicinity of quantum critical point, the competition of the two different excitation mechanisms results in critical behaviors aforementioned, and detailed study of these behaviors are carried out in specific systems.

DOI: 10.54254/2753-8818/19/20230517

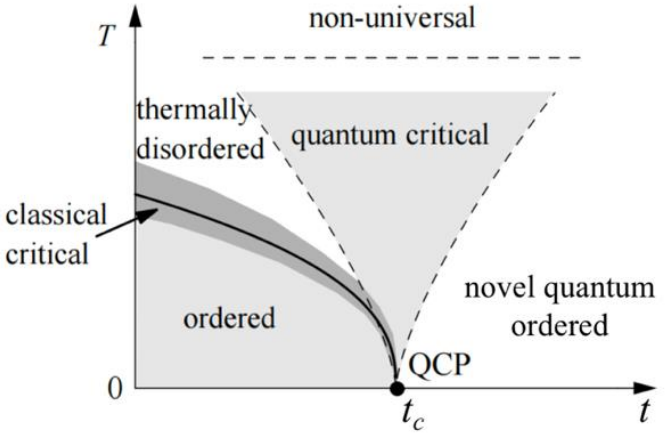


**Figure 2.** Schematic phase diagrams near the quantum critical point (QCP). Long-range order is destroyed by thermal or quantum fluctuations respectively in different regions. In the quantum critical region, the physics is controlled by the thermal excitations of the quantum critical ground state. $T$ refers to temperature of the considered system, and $t$ is the external tuning parameter, with subscript c characterizing the quantum critical point. This figure is adjusted from [10].

*1.1.1. Quantum criticality in ferroelectrics.* QPT is most studied in antiferromagnetic (AFM) systems. The occurrence of spontaneous magnetism requires the constituent electrons to have a net angular momentum [11]. And magnetization arises from either spin-orbit coupling, or quantum-mechanical exchange energy, or both. One typical system where ferromagnetic (FM) QPT takes place is the dimer antiferromagnet realized in $TlCuCl_3$. Its unit cell is shown in figure 3 (a), where unpaired spins are localized on each $Cu^{2+}$ ion. The Hamiltonian describing the spins $\boldsymbol{S_i}$ at 0K could be written as:

$$\mathcal{H} = \sum_{i<j} J_{ij} \boldsymbol{S_i} \cdot \boldsymbol{S_j} \tag{1.1}$$

where $J_{ij}$ is the exchange coupling between the $i$th and the $j$th site. Due to energy minimization, the ground state of the system has anti-parallel (Neel order) spins [12]. For sufficient low $T$, either side of QCP could be described by low-lying excitations of the ground states, as is shown in figure 3 (b, c). In $g < g_c$ region, spin waves with strong non-linear couplings destroy the Neel order at all $T > 0$, while in $g > g_c$, the excitations are the triplet excited states of each dimer [12].

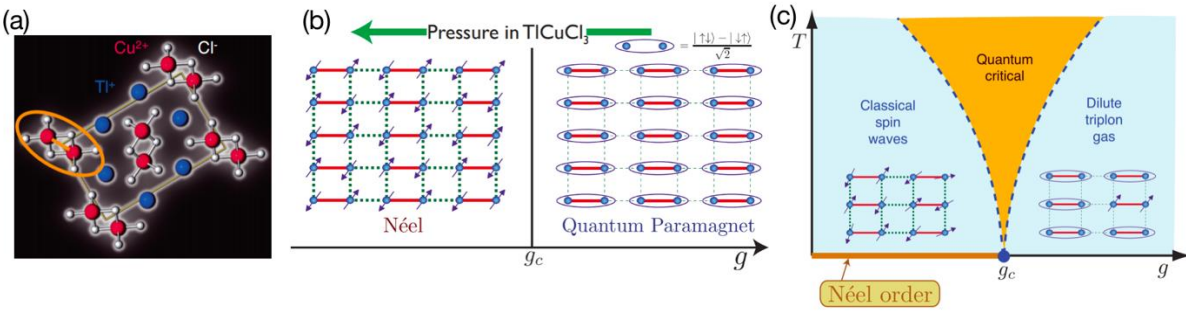


**Figure 3.** QPT in an AFM System $TlCuCl_3$. (a) The unit cell of insulating antiferromagnet (AFM) $TlCuCl_3$. (b) A schematic of tuning external field for dimer antiferromagnet. The solid lines represent the exchange interaction $J > 0$, while the dashed lines have exchange $J/g$ with $g > 1$. The singlet valence bond of spins $(|\uparrow\downarrow\rangle - |\downarrow\uparrow\rangle)/\sqrt{2}$ forms when $g > g_c$ and the system transits into a quantum paramagnetic phase. (c) Phase diagram at low $T$. QPT influences the behaviors of the system even when temperature is not precisely 0K. The most direct and also most significant manifestation of these influences is the emergence of the quantum critical region. This figure is taken from [12].

In the corresponding case of ferroelectricity (FE), it is related to the spontaneous electric polarization $P(\boldsymbol{r})$ that could be reversed by external electric field. A good example of studying FE is the $ABO_3$ perovskite family, and the stereotype structure is shown in figure 4 (a). As is shown in figure 4 (b), the existence of local $P(\boldsymbol{r})$, i.e., inhomogeneous distribution of positive and negative charge, is determined

DOI: 10.54254/2753-8818/19/20230517

by the small shift of B cation at the cubic center. Moreover, whether or not these local distortions $P(\boldsymbol{r})$ line up to form FE state depends on dipole-dipole interaction, analogous to the exchange effect in FM case. A comparison between FM and FE are listed in table 1.

**Table 1.** A brief comparison between FM and FE.

| | Ferromagnetism | Ferroelectricity |
|---|---|---|
| **Dipole moment** | Spontaneous magnetization | Spontaneous electric polarization |
| **Origin of dipole moment** | Intrinsic spin angular momentum | Charge asymmetry |
| **Origin of anisotropy** [4] | Spin–orbit coupling | Crystal electric field |
| **Magnitude of dipole interaction** | Relatively strong Coulomb force | Relatively weak Ampère force |
| **Phase transitions** [4] | Often second-order, non-mean field behavior observed | Often first-order, non-mean field behavior rare |
| **External tuning parameter** | Applied magnetic field | Applied electric field |
| **Description of polarization** | Susceptibility | Permittivity |
| **Possible applications** | Transducer, actuator, due to relatively strong piezoelectric effect | Magnetic tape, data storage, due to hysteresis effect |

The transition between paraelectricity (PE) and FE involves two types, the displacive type and the order-disorder type, as shown in figure 5 (a, b). Displacive phase transition refers to the collective displacements of atoms, whose arrangement at the ground state yields no local polarization, i.e., $P(\boldsymbol{r}) = 0$. Therefore, the bulk average $P_s \equiv \langle P(\boldsymbol{r}) \rangle$ is zero, and this state is defined as PE. When $T$ rises, $P(r)$ align in the same direction and the system has a net polarization, turned into the FE phase. The order-disorder type, on the other hand, has the same FE state. However, there exists local polarization within each formation unit and the macroscopic PE state is due to the cancelling of lattice polarization, i.e., $P(\boldsymbol{r}) \neq 0, P_s = 0$.

In a classical $T$-driven phase transition, FE exists under the Curie temperature $T_c$, above which the material becomes paraelectric. However, FE-PE transition could also be tuned at 0K by tuning parameters such as applied electric field, as shown in figure 5 (c). Hence, the balance of thermal and quantum fluctuations at low $T$ expands QCP to a critical region [3] where emergent phenomena is still under investigation.

DOI: 10.54254/2753-8818/19/20230517

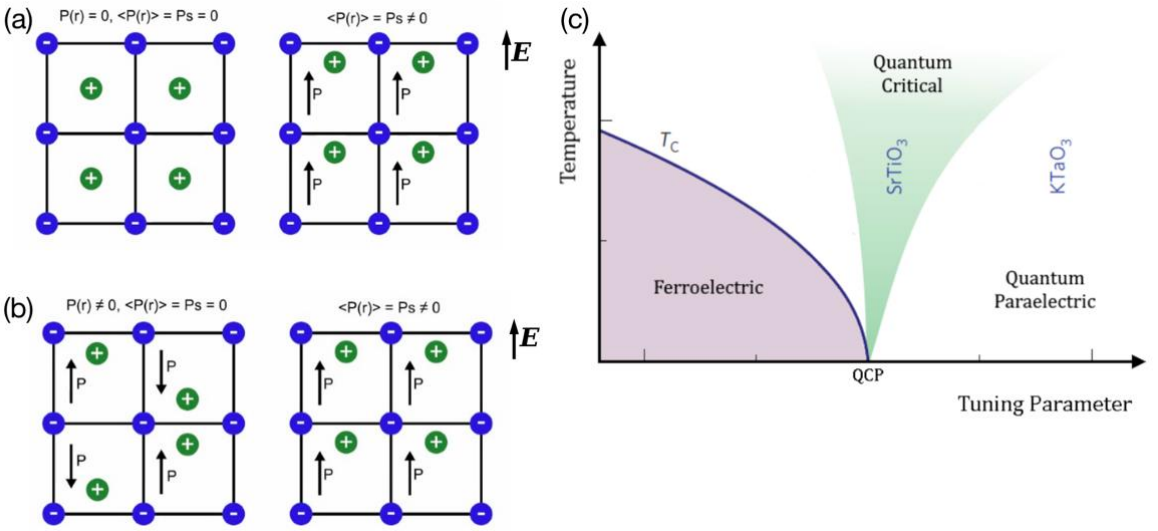


**Figure 5.** Two types of PE-FE phase transition and the phase diagram. (a) Displacive phase transitions. Small collective displacements of individual atoms shift the polarization of the lattices from $P(\boldsymbol{r}) = 0, P_s \equiv \langle P(\boldsymbol{r}) \rangle = 0$, i.e., consisting neither local nor spontaneous electric dipole, to $P_s \neq 0$. (b) Order-disorder phase transitions. It is characterized by disorder of the atoms or molecules in the structure of one of the phases, $P(\boldsymbol{r}) \neq 0, P_s = 0$ for instance. (c) Phase diagram for displacive ferroelectric materials [13]. As $g \equiv |\boldsymbol{E}|$ increases, the FE order is destroyed at QCP where dipole interactions diverge into large length scales. At low $T$, the balance between quantum and thermal fluctuations determines the FE or quantum-PE phases, and the critical region that separate them.

*1.1.2. The focus of this report.* We choose strontium titanite oxide $SrTiO_3$ (STO) as the subject system to further explore the nature of ferroelectric quantum criticality. STO is an ideal, clean model system for exploring quantum paraelectricity [14]; Besides, due to the crystal structure, it stays close to the QCP (as shown in figure 5 (c)), which enables relatively easy tuning in comparison with other perovskites like potassium tantalum oxide $KTaO_3$. The measurements of relative dielectric permittivity via inelastic neutron scattering, Raman scattering and other techniques show that FE fails to emerge below $T_c$, i.e., the system remains paraelectric. The interpretation of this quantum critical behavior, known as incipient ferroelectricity, requires both phenomenological theory and lattice dynamics.

*1.2. Phenomenological description*

Many attempts have been made trying to describe phase transitions without the confinement to particular types of materials. In 1937, Landau derived a theory based on the degrees of freedom and symmetries of the system [15]. As a result of cooling or other external parameters, the degree of symmetry lowers, and therefore the system transits to another phase. In order to quantify this emergence of long-range order, Landau introduced the order parameter (OP) $\phi$. $\phi = 0$ is related to the disordered state with higher degree of symmetry, while $\phi \neq 0$ corresponds to the ordered state with lower degree of symmetry. In the case of ferroelectric phase transition, $\phi$ turns out to be the dipole moment [16], proportional to the polarization. When the system is paraelectric above $T_c$, dipole moments of each lattice site point to arbitrary directions without $\boldsymbol{E}$, and therefore $\phi = 0$; After cooling below $T_c$, however, $P(\boldsymbol{r})$ emerges and thus indicates that $\phi \neq 0$.

*1.2.1. Landau theory and critical behaviours.* The method Landau applied is to replace the many-body interaction by the interaction with a mean field that captures average behaviors of surrounding sites. This approximation, known as the mean field theory (MFT), neglects local fluctuations and simplifies the Hamiltonian $\mathcal{H}$ of the system. The simplest model to apply MFT is the Ising model proposed by

DOI: 10.54254/2753-8818/19/20230517

Ernst Ising. It consists of a lattice of "spin" variables $\sigma_i$ which could only be $+1$ (up) or $-1$ (down). Besides, $\sigma_i$ could only interact with sites directly adjacent to it [17].
In Ising model, the Hamiltonian is:

$$\mathcal{H} = -h\sum_j \sigma_j - J\sum_{<ij>} \sigma_i\sigma_j \tag{1.2}$$

where the first term describes the interaction with the external field $h$ and the latter characterizes the interactions between sites. Then consider MFT in which OP is defined as

$$\phi \equiv \frac{1}{N}\sum_{i=1}^{N} < \sigma_i > \tag{1.3}$$

where

$$< \sigma_i > \equiv \frac{Tr\left(\sigma_i e^{-\beta\mathcal{H}}\right)}{Z} \tag{1.4}$$

denotes the mean value of the spin variables, $\beta = \frac{1}{k_B T}$ and $Z \equiv Tr\left(e^{-\beta\mathcal{H}}\right)$ represents the thermodynamic quantities of the system. Replace the right side of equation (1.2) with equation (1.3) and equation (1.4), we arrive at the equation that OP must follow:

$$\phi = \tanh[\beta(h + mJ\phi)] \tag{1.5}$$

where $m$ represents the number of nearest neighbors. The solution of equation (1.5) leads to the critical temperature

$$T_c = \frac{mJ}{k_B} \tag{1.6}$$

and the states of the system above or below it, as shown in figure 6.

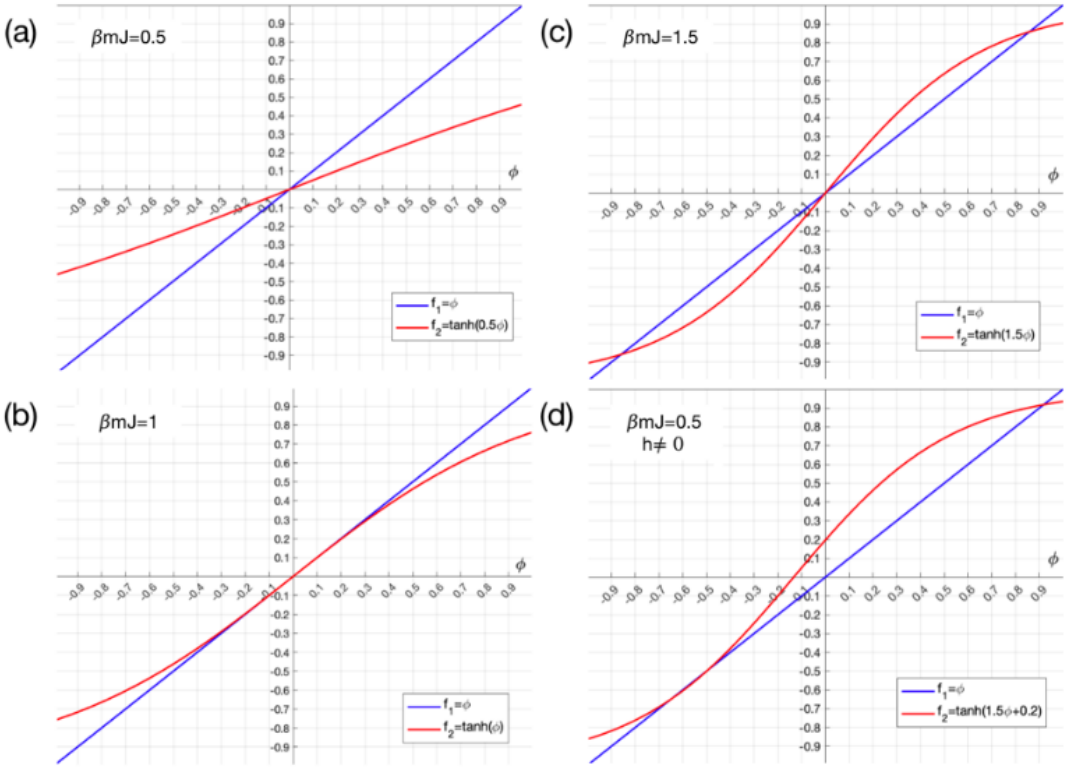


**Figure 6.** Schematic solution of equation (1.5). The intersections of two curves $f_1$ and $f_2$ represent possible value OP could take. As plotted in (a) and (b), two curves intersect at $\phi = 0$ only, as long as $\beta mJ \leq 1$, or $T \geq mJ/k_B$. This indicates that the system could only be PE. However, in the region

DOI: 10.54254/2753-8818/19/20230517

where $\beta mJ > 1$, or $T < mJ/\mathrm{k_B}$, equation (1.5) has three solutions with two non-zero value of $\phi$. In this case, further calculations of energy density are required to determine the value of OP of the system. Therefore, the critical temperature of the system is $T_\mathrm{c} = mJ/\mathrm{k_B}$. If external field $h$ is applied, $f_2$ will shift and thus change the intersections.

Another important assumption in Landau theory is that in the vicinity of the critical point, free energy density $f$ as the function of $\phi$

$$f(\phi) \equiv -\mathrm{k_B}T \ln Z \tag{1.7}$$

is analytic. Therefore, if the external field is absent, i.e., $h = 0$, then

$$\begin{aligned} f(\phi) &= \frac{NqJ}{2}\phi^2 - N\mathrm{k_B}T \ln 2 - Nk_BT \ln\,[\cosh(\beta h + \beta mJ\phi)] \\ &= -N\mathrm{k_B}T \ln 2 + \frac{N\mathrm{k_B}T_\mathrm{c}}{2T}(T - T_\mathrm{c})\phi^2 + \frac{N\mathrm{k_B}T_\mathrm{c}^4}{12T^3}\phi^4 + \mathcal{O}(\phi^6) \\ &= f_0 + a(T - T_\mathrm{c})\phi^2 + b\phi^4 + \mathcal{O}(\phi^6) \end{aligned} \tag{1.8}$$

where $f_0 = -N\mathrm{k_B}T \ln 2$ is the overall energy shift, and $a = N\mathrm{k_B}T_\mathrm{c}/2T$ , $b = N\mathrm{k_B}T_\mathrm{c}^4/12T^3$ are positive constants. In terms of the equilibrium state, as is shown in figure 7 (a, b), it is clear that when $T > T_\mathrm{c}$, $f$ minimizes at $\phi = 0$, indicating that thermal fluctuations force the system to be disordered. By contrast, when $T$ approaches $T_\mathrm{c}$ from below, the order parameter takes non-zero value at $f = f_\mathrm{min}$:

$$\phi_0 = \pm\left(\frac{a(T_\mathrm{c} - T)}{2b}\right)^{1/2} \tag{1.9}$$

Therefore, as the temperature drops, the system undergoes a spontaneous symmetry breaking with $\phi \propto (T_\mathrm{c} - T)^{1/2}$ (figure 7 (c)), and the energy density of the system changes continuously with $T$ (figure 7 (d)).

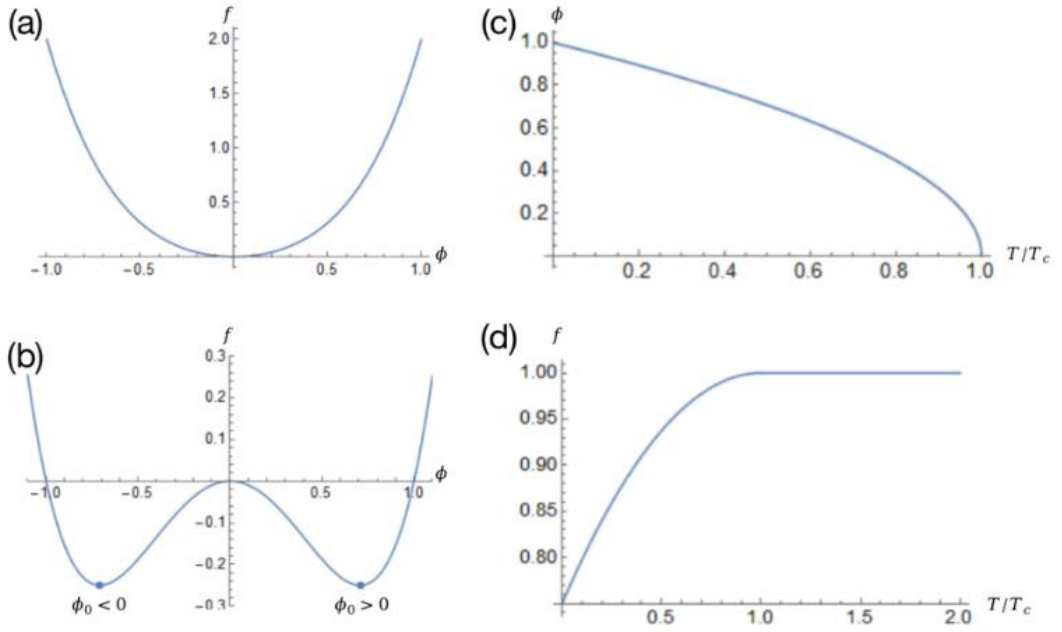


**Figure 7.** $\phi$ dependence of free energy density and temperature dependence of OP under MFT Ising model without applied field. (a) When $T > T_\mathrm{c}$, Helmholtz free energy density minimizes only in the disordered phase. (b) When $T < T_\mathrm{c}$, the system stabilizes at two symmetrically placed, nonzero OP. Hence, the system undergoes a phase transition, i.e., symmetry breaking, when temperature drops. (c) Temperature dependence of OP below the critical point. (d) Temperature dependence of energy density $f$ which changes continuously as $T$ drops.

DOI: 10.54254/2753-8818/19/20230517

By further investigating the derivatives of $\phi$ and $f$, we arrive at several critical behaviors, a.k.a. power laws, characterized by critical exponents. For instance, the susceptibility $\chi$ (which is related to relative dielectric permittivity $\varepsilon$ by $\varepsilon(T) = 1 + \chi(T)$) is defined as

$$\chi(T,h) \equiv \left(\frac{\partial \phi}{\partial h}\right)_T \tag{1.10}$$

Apply equation (1.5) under the absence of external field, $\varepsilon$ turns out as

$$\chi(T,h=0) = \frac{\beta}{\cosh^2[\beta(h+mJ\phi] - \beta mJ} \tag{1.11}$$

When $T$ approaches $T_c$ from below, OP takes the value of $\phi_0$ in equation (1.9). Hence,

$$\begin{aligned} \lim_{T\to T_c^-} \chi(T,h=0) &= \frac{\beta}{1+3(\beta mJ)^2|t| - \beta mJ} \\ &\approx \frac{1}{2k_B T_c} \cdot \frac{1}{|t|} \end{aligned} \tag{1.12}$$

where the reduced temperature $t \equiv \frac{T-T_c}{T_c}$ in temperature-induced phase transitions. On the contrary, when $T$ approaches $T_c$ from above, $\phi = 0$, and

$$\begin{aligned} \lim_{T\to T_c^+} \chi(T,h=0) &= \frac{\beta}{1-\beta mJ} \\ &= \frac{1}{k_B T_c} \cdot \frac{1}{|t|} \end{aligned} \tag{1.13}$$

From equation (1.12) and equation (1.13), we define $\gamma = -1$ in MFT approximation, and then $\chi$, or $\varepsilon$, diverges as

$$\varepsilon(T) \sim |T - T_c|^{-\gamma} \tag{1.14}$$

at the critical point, as shown in figure 8 (a). Similar analysis of the specific heat $c_v \equiv -T\frac{\partial^2 f}{\partial T^2}$ shows that $c_v$ experiences a "jump" at the critical point, as is shown in figure 8 (b). More detailed calculations of other critical exponents are provided in [18].

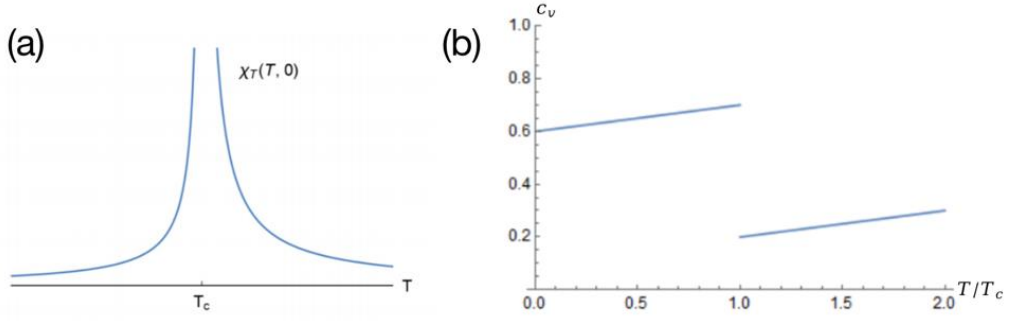


**Figure 8.** Two critical behaviours under MFT Landau theory. (a) Temperature dependence of susceptibility $\chi$. Relative permittivity $\varepsilon \equiv 1 + \chi$. The inverse power law gives Curie-Weiss relation of susceptibility above $T_c$. The divergence of $\varepsilon$ leads to the correction of Landau theory. This figure is adjusted from [19].

*1.2.2. Dimensionality and quantum extrapolation.* The nonanalyticity of susceptibility shown in figure 8 (a) is not physically plausible. These two conclusions are inconsistent with observations of fluctuations near $T_c$. Besides, as is deduced from equation (1.2), dimensionality, exponentially related to the degrees of freedom of Hamiltonian $\mathcal{H}$, has little effect in determining when the system stabilizes. This is because we only need to adjust the range of summation if we generalize Ising model to many-body interactions.

Ginzburg first addressed the dimensionality effect on phase transitions. In order to describe the extent of correlation among local OP fluctuations, correlation length $\xi$ is introduced. In the 1D Ising model aforementioned, $\xi$ is calculated as

DOI: 10.54254/2753-8818/19/20230517

$$\xi = -\frac{1}{\ln \tanh(\beta J)} \tag{1.15}$$

Moreover, another critical exponent $\nu$ is defined to characterize the divergence near $T_c$, so that $\xi \propto |t|^{-\nu}$ where $\nu = 1/2$ in MFT approximation. Further investigation leads to a quantitative determination of when fluctuations are nonnegligible,

$$\xi^{4-d} \ll \frac{\kappa^2}{4c} \tag{1.16}$$

where $d$ is the spatial dimensionality and $\kappa^2/4c$ is a constant determined by the symmetry of the system. This criterion given by Ginzburg-Landau (GL) theory tells that despite the type of system considered, $\xi$ diverges when $d < 4$. It indicates that fluctuations could not be neglected in any effective approach in $d < d_0$ [15]. This dimension $d_0 = 4$ is called the upper critical dimension for $\phi^4$.

Our discussion is hitherto limited to classical statistical-mechanical models [20] where $T_c$ is finite. If $T_c = 0$, however, the tuning parameter becomes temperature- independent. Moreover, at sufficiently low $T_c$, due to the coexistence as well as the competition of thermal and quantum fluctuations, it is vital to determine which of the two physically different mechanisms dominates critical behaviors, especially near the quantum critical point. In general terms, quantum mechanics will be important as long as the typical energy scale is far larger than the thermal energy [18]. A more thorough and quantum-generalized analysis is given by Rechester *et al* [21].

The quantum generalization of GL theory, the $\phi^4$-quantum field model, includes an extra temporal dimension with OP being expressed in $\phi(r, \tau)$, where $\tau$ is an imaginary time within a finite range $0 < \tau < \hbar k_B T$ [6]. Correspondingly, the dimension $d$ in Ginzburg criterion is now an effective one: $d_{\text{eff}} \equiv d + z$, where $z$ is the dynamical exponent. With self-consistent field approximation being applied to this model, the criticality of $\varepsilon$ for instance, follows a non-classical temperature dependence where the exponent $\gamma$ is now calculated to be $\gamma = (d_{\text{eff}} - 2)/z$ at critical point as long as $d_{\text{eff}} > 4$.

### *1.3. Phonon modes*

The relation between relative permittivity $\varepsilon$ and temperature $T$ described in equation (1.14) could also be given from lattice dynamics, alternatively understood as phonons. Lyddane, Sachs and Teller derived a relation between phonons and the dielectric response of a polarizable crystal [22]:

$$\frac{\varepsilon_0}{\varepsilon_\infty} = \frac{\omega_{\text{LO}}^2(0)}{\omega_{\text{TO}}^2(0)} \tag{1.17}$$

where $\varepsilon_0$ stands for static permittivity, $\varepsilon_\infty$ is the refractive index, and the subscript LO and TO refers to the longitudinal and transverse optic mode. In equation (1.16), the dispersion relation $\omega = \omega(\boldsymbol{q}) = \omega(0)$ refers to the low-lying, temperature-dependent optic mode at the center of Brillouin Zone (BZ) [22]. This mode is called the soft mode, which results in OP ordering in FE systems.

According to Cochran, $\omega_{\text{TO}}^2(T) \propto |T - T_c|$ when transition is approached and reaches zero at the transition point [23], i.e., the mode "softens". Therefore, combining this relation with equation (1.17), we arrive at

$$\varepsilon_0 \propto |T - T_c|^{-1} \tag{1.18}$$

which is experimentally summarized by Curie and Weiss. Besides, the singularity in equation (1.18) is in consistence with equation (1.14) in MFT Landau theory.

The LST relation is deduced under harmonic approximation [24]. However, the effect of phonon coupling and their mutual energy exchange could not be overlooked at sufficiently low $T$. Detailed analysis of higher order expansions of the energy potential leads to the quantum field theory of phonons, much of which was established by Cowley, Kadanoff [25] and Baym *et al* [26]. The technique vigorously solves the self-energy of phonons and predicts measurable signatures of anharmonicity: real frequency shifts and linewidth broadening [27]. Besides, it yields the temperature dependence of relative permittivity at frequencies below TO mode, applying the generalization of LST relation to the quantum-dominated region.

DOI: 10.54254/2753-8818/19/20230517

## 2. Quantum criticality in strontium titanate

Strontium titanate oxide (STO) has attracted a lot of attention in terms of critical behaviors. Previous studies of quantum criticality in STO involve the measurement of quantum critical fluctuations on soft mode that is temperature and pressure dependent [28], the stabilization of FE phase via irradiation with an off-resonant strong phonon field [14], the verification of MFT-like pressure dependence of the stiffening of soft phonon [24], the competition between PE and SC due to chemical doping (Ca, $^{18}O$, etc.) [14], etc. What lies behind these critical behaviors is the competition and coupling of different forces, modes and interaction patterns.

### *2.1. Critical behaviors near quantum critical point*

In STO, FE condensation never appears at the critical point predicted by equation (1.18) where $T_c \sim 38\ K$. From the perspective of phonon modes, the long-range FE order originates from a doubly degenerate Γ point TO mode [[31]] that falls to zero at $T_c$, driving the oxygen octahedron and titanium ions rotating in the opposite directions. Therefore, the suppression of FE indicates the flattening of phonon frequency to around 10 $cm^{-1}$, suggesting the nearby QCP.

Moreover, the dielectric constant, as is verified through inelastic neutron scattering (INS) by Yamada *et al*. [30] and Raman scattering by Fleury and Worlock [31], deviates from the classical behavior below 50K and experiences $T^{-2}$ temperature dependency, followed by anomalous upturns below a few kelvin [4]. This incipient FE instability could be explained via $\phi^4$-quantum field model under self-consistent approximation, with logarithmic correction (related to the electrostrictive effect) taken into consideration.

### *2.2. $\boldsymbol{\phi^4}$-theory for quantum phase transition*

The $\phi^4$ quantum field theory explains non-classical behaviors in the vicinity of QCP ($T_c = 0$) and predicts emergent phenomena in the quantum critical region. When $k_B T \sim \hbar\omega$, quantum fluctuations have to be taken into consideration. In this case, each vibration mode with wavevector $\boldsymbol{q}$ depends not only on temperature but also on the dynamical properties. More generally, each mode has a distribution of frequencies that results in a statistical mechanical description involving not only the sum over wavevectors ($d$ dimensions in real space) but also over phonon frequency $\omega_q$ [7]. Therefore, the dynamical exponent $z$ in the low-$q$ dispersion relation $\omega \propto q^z$ is included in the quantum generalization of GL theory. Our goal is to derive the temperature dependence of relative permittivity $\varepsilon(T)$ or susceptibility $\chi(T)$, and calculate the critical exponent $\gamma$ under quantum approach.

*2.2.1. Effective dimension.* According to 1.2, the fluctuation of OP could be written as:

$$\delta\phi \equiv \phi - \langle\phi\rangle \tag{2.1}$$

and we assume that Langevin field drives the thermal and quantum fluctuations, i.e., $\langle\delta\phi\rangle = 0$. The severity of local fluctuations could be described with the variance of $\phi$ [7]:

$$\langle\delta\phi^2\rangle = \frac{2}{\pi}\sum_{q<q_c}\int_0^\infty d\omega\left(n_\omega + \frac{1}{2}\right)\mathrm{Im}\,\chi_{q,\omega} \tag{2.2}$$

where $q_c$ limits the summation over states, $n_\omega$ satisfies the Bose-Einstein distribution as $n_\omega = 1/[\exp(\hbar\omega/k_B T) - 1]$. According to the fluctuation-dissipation theory, the link between the variance of amplitude fluctuations and the imaginary part of the response is

$$\mathrm{Im}\,\chi_{q,\omega} = \frac{\pi}{2}\omega\chi_q\delta(\omega - \omega_q) \tag{2.3}$$

Therefore, if $k_B T \gg \hbar\omega$, all the states within BZ are excited and equation (2.2) is approximated to be

$$\langle\delta\phi^2\rangle \approx T\sum_{q<q_{BZ}}\chi_q \tag{2.4}$$

DOI: 10.54254/2753-8818/19/20230517

This is the classical limit where thermal fluctuations dominate the behaviors of the system and statistical properties could be derived via $d$-dimension integration. However, if $k_B T \ll \hbar\omega$, $q_c$ should be temperature-dominated and therefore satisfies the relation $q_c \equiv q_T \propto T^{1/z}$. Hence,

$$\langle \delta\phi^2 \rangle \approx T \sum_{q<q_T} \chi_q \tag{2.5}$$

In order to determine the state when external field $h$ is applied, we rewrite equation (1.8) as:

$$f = \frac{1}{2}\alpha\phi^2 + \frac{1}{4}\eta\phi^4 + \frac{1}{2}\zeta|\nabla\phi|^2 - h\phi \tag{2.6}$$

where $f_0$ is set to be zero and it is assumed that $\phi$ varies slowly in space. $\alpha, \eta, \zeta$ are three parameters whose physical interpretations will be discussed in subsection 2.2. Comparing equation (1.8) with equation (2.5), it is evident that $\alpha = 2a(T - T_c) = 2aT$ and thus in the vicinity of QCP, $\alpha \to 0$. Follow the similar approach in subsection 1.2.1, we minimize the free energy and arrive at

$$h = \alpha\phi + \eta\phi^3 - \zeta\nabla^2\phi \tag{2.7}$$

Apply equation (2.1) and the assumption $\langle \delta\phi \rangle = 0$, equation (2.7) is rewritten as

$$h = (\alpha + 3\eta\langle \delta\phi^2 \rangle)\langle \phi \rangle + \zeta\nabla^2\langle \phi \rangle \tag{2.8}$$

where $3\eta\langle \delta\phi^2 \rangle\langle \phi \rangle$ is the influence of anharmonicity in equation (2.6). Recall equation (1.5) and the definition (1.10), and substitute the external field with equation (2.8), it yields:

$$\chi_q^{-1} = (\alpha + 3\eta\langle \delta\phi^2 \rangle) + q^2 \tag{2.9}$$

where $[\alpha + 3\eta\langle \delta\phi^2 \rangle]$ is related to the correction length [8]. Therefore, we find that

$$\chi_q^{-1} \propto \kappa^2 + q^2 \tag{2.10}$$

where $\kappa \equiv 2\pi/\xi$ is the correlation wavevector. In the long-wavelength limit, i.e., $q \to 0$,

$$\chi_q^{-1} \propto \kappa^2 \tag{2.11}$$

Now combine equation (2.11) with equation (2.5), we arrive at the self-consistent equation for the correlation wavevector

$$\kappa^2 \propto \sum_{q<q_T} \frac{T}{\kappa^2 + q^2} \approx T \int_0^{q_T} dq \frac{q^{d-1}}{\kappa^2 + q^2} \approx T q_T^{d-2} \left[1 - \left(\frac{\kappa}{q_T}\right)^{d-2}\right] \tag{2.12}$$

If we neglect $(\kappa/qT)^{d-2}$on the right side of equation (2.12), we get the temperature dependence of susceptibility mentioned briefly in subsection 1.2.2:

$$\chi^{-1} \propto T^{\gamma} \tag{2.13}$$

where the critical exponent is defined as $\gamma \equiv (d_{\text{eff}})/z = (d + z - 2)/z$.

However, the simplification that results in equation (2.13) is qualified under the condition $d_{\text{eff}} > 4$, since

$$\left(\frac{\kappa}{q_T}\right)^2 \propto T^{\frac{d+z-4}{z}} \left[1 - \left(\frac{\kappa}{q_T}\right)^{d-2}\right] \tag{2.14}$$

and $d + z > 4$ is the only circumstance that enables $\frac{\kappa}{q_T} \to 0$ when $T \to 0$. Therefore, on the marginal dimension, or the upper critical dimension $d_{\text{eff}} = 4$, terms after the second approximation in equation (2.12) are no longer valid. Solving the self-consistency equation in this particular case yields a logarithmic correction of equation (2.13), which explains the upturn of $\varepsilon \sim T^{-1}$ diagram below 4K [4].

*2.2.2.* $\boldsymbol{\phi^4}$ *- Approach in strontium titanate.* When we apply the aforementioned self-consistent approximation of $\phi^4$- quantum field theory into PE-FE phase transition in STO system, the parameters $\alpha$ and $\eta$ in equation (2.6) are calculated under spatially-invariant polarization field, and thus could be set from the linear relation between $h/\phi$ and $\phi^2$:

$$\frac{\mathcal{E}}{P} = \alpha + \eta P^2 \tag{2.15}$$

where the external field $h$ is the tunable electric field $\mathcal{E}$ and OP $\phi$ is proportional to the polarization $P$. Besides, $\alpha$ represents the inversion of static susceptibility multiplied by static permittivity, while $\eta$ is the mode-mode coupling parameter that shows the anharmonicity near QCP. Meanwhile, $\zeta$ stands for

DOI: 10.54254/2753-8818/19/20230517

the stiffness of phonon modes and is related to the excitation gap $\Delta$ as well as the group velocity $v$: $\zeta = \alpha^2 v^2/\Delta^2$. The relatively small $\alpha$ and $\Delta$ in STO implies that it is close to displacive ferroelectric QCP, in accord with figure 5 (c).

## 3. Summary

In this report, quantum criticality is firstly introduced in a general picture and then specified in antiferromagnetic and ferroelectric systems respectively. In order to explain the absence of paraelectric – ferroelectric phase transition in strontium titanite oxide, a detailed analysis of Landau theory and critical behaviors is demonstrated, followed by an equivalent description in the form of soft phonon modes that yields temperature dependence of the relative permittivity. Besides, a qualitative quantum field interpretation, i.e., $\phi^4$ quantum field theory, is deduced and applied to electric-field driven quantum phase transition. This model interpretates the $\varepsilon \sim T$ relation with temperature below the Curie point $T_c \sim 38\mathrm{K}$, and taking electrostrictive effect into consideration in the self-consistent equation explains the upturn of $\varepsilon \sim T^{-1}$ relation measured around 2K.

## References


[1] Zhang Z *et al* 2021 *Phys. Rev.* B 103 22
[2] Andres J *et al* 2012 *Photoluminescence: Applications, Types and Efficacy* 119-61
[3] Rowley S E *et al* 2014 *Nat. Phys.* 10 367
[4] Spaldin N A 2007 *Topics Appl. Phys.* 105 175
[5] Wang K 2021 Landau's theory of phase transition *Archived*
[6] Lyddane R H, Sachs R G and Teller E 1941 *Phys. Rev.* 59 673
[7] Morice C, Chandra P, Rowley S E, Lonzarich G and Saxena S 2017 *Phys. Rev.* B 96 245104
[8] Ahmed R *et al* 2021 Results Phys. 20 103623
[9] Seki Y, Tanaka S and Kawabata S 2019 *J. Phys. Soc. Jpn.* 88 054006
[10] Vojta M 2003 *Rep. Prog. Phys.* 66 2069
[11] Sachdev S *et al* 2011 *Phys. Today* 64 29
[12] Burdett J K 1981 *Inorg. Chem.* 20 1959
[13] Zhong W and Vanderbilt D 1995 *Phys. Rev. Lett.* 74 2587
[14] Yamada Y and Shirane G 1969 *J. Phys. Soc. Jpn.* 26 396-403
[15] Cochran W 1959 *Phys. Rev, Lett.* 3 412
[16] Hertz J A 1976 *Phys. Rev.* B 14 1165
[17] Fendley P 2014 *Modern Statistical Mechanics* (Virginia: The University of Virginia)
[18] Callen H 1991 *Thermodynamics and an Introduction to Thermostatistics* (NY: Wiley)
[19] Khmel'nitskii D E and Shneerson V L 1972 *J. Exp. Theor. Phys* 37 164
[20] Sachdev S 1999 *Quantum Phase Transitions* (Cambridge: Cambridge University Press)
[21] Feder J and Pytte E 1970 *Phys. Rev.* B 1 4803
[22] Kuzmanovski D *et al* 2022 Kapitza stabilization of a quantum critical order *arXiv e-prints* https://doi.org/10.48550/arXiv.2208.09491
[23] Edge J M *et al* 2015 *Phys. Rev. Lett.* 115 247002
[24] Kadanoff L P and Baym G 1962 *Quantum Statistical Mechanics: Green's Function Methods in Equilibrium and Nonequilibrium Problems* (NY: CRC Press)
[25] Taniguchi H, Itoh M and Yagi T 2007 *Phys. Rev. Lett.* 99 017602
[26] Born M and Oppenheimer J R 1927 *Annelen der Physik* 389 457
[27] Coak M J *et al* 2019 *Phys. Rev.* B 100 214111
[28] Rowley S E *et al* 2011 *Low Temp. Phys.* 37 2–7
[29] Chandra P, Lonzarich G G, Rowley S E and Scott J F 2017 *Rep. Prog. Phys.* 80 112502
[30] Worlock J M and Fleury P A 1967 *Phys. Rev. Lett.* 19 1176
[31] Pytte E and Feder J 1968 *Phys. Rev.* 168 640